

Incremental Learning of Structured Memory via Closed-Loop Transcription

Shengbang Tong¹ Xili Dai^{1,2} Ziyang Wu³ Mingyang Li⁴ Brent Yi¹ Yi Ma^{1,4}

Abstract

This work proposes a minimal computational model for learning a structured memory of multiple object classes in an incremental setting. Our approach is based on establishing a *closed-loop transcription* between multiple classes and their corresponding subspaces, known as a linear discriminative representation, in a low-dimensional feature space. Our method is both simpler and more efficient than existing approaches to incremental learning, in terms of model size, storage, and computation: it requires only a single, fixed-capacity autoencoding network with a feature space that is used for both discriminative and generative purposes. All network parameters are optimized simultaneously without architectural manipulations, by solving a constrained minimax game between the encoding and decoding maps over a single rate reduction-based objective. Experimental results show that our method can effectively alleviate catastrophic forgetting, achieving significantly better performance than prior work for both generative and discriminative purposes.

1. Introduction

Artificial neural networks have demonstrated a great ability to learn representations for hundreds or even thousands of classes of objects, in both discriminative and generative contexts. However, networks typically must be trained offline, with data sampled from *all classes simultaneously*. When a network is naively retrained to learn new classes without data from the old ones, previously learned knowledge will fall victim to the problem of *catastrophic forgetting* (McCloskey & Cohen, 1989). This is known in neuroscience as the *stability-plasticity dilemma*: the challenge of ensuring that a neural system can learn from a new environment while retaining essential knowledge from previous ones (Grossberg, 1987).

¹University of California, Berkeley, CA, USA ²University of Electronic Science and Technology of China, China ³International Digital Economy Academy (IDEA), Shenzhen, China ⁴Tsinghua-Berkeley Shenzhen Institute (TBSI), Tsinghua University, China. Correspondence to: Yi Ma <yima@eecs.berkeley.edu>.

In contrast, natural neural systems like those found in animal brains do not seem to suffer from such catastrophic forgetting at all. They are capable of learning from new objects while preserving their memory of previously learned objects. This ability, for either natural or artificial neural systems, is often referred to as *incremental learning*, *continual learning*, *sequential learning*, or *life-long learning* (Allred & Roy, 2020). Emulating this capability would enable artificial neural systems that are trained in fundamentally more scalable and flexible ways, for example, without preparing or providing data for many classes all at once.

Many recent works in the neuroscience and machine learning communities have highlighted the importance of this problem, leading to methods for training neural networks with external mechanisms for addressing the stability-plasticity dilemma. These mechanisms include retaining raw exemplar data (Rebuffi et al., 2017), maintaining a separate generative neural network (Shin et al., 2017), or performing architectural manipulations (Mallya & Lazebnik, 2018). Inspired by the more fundamental propensity for learning incrementally that we see in natural neural systems, our work studies incremental learning with a focus on circumventing the complexity of these external mechanisms. We present a combination of two qualities, which have not been demonstrated in conjunction in existing incremental learning approaches:

- **Memory-based.** When learning new classes, raw exemplars of old classes are difficult to scale, and should not be relied on to train the network together with new data. An alternative is a compact *memory* of old classes to use for replay, such as one represented by a generative feature space, as well as the associated encoding and decoding mappings (Kemker & Kanan, 2018).
- **Self-contained.** Incremental learning should take place on a self-contained neural system, as a brain, with a *single representation space* and a *fixed capacity*. The ability to minimize forgetting should be implied by optimizing an overall learning objective itself, without relying on an external generative model for reply or external mechanisms for architectural modification and resource allocation,¹ which often require additional

¹As to be surveyed in Section 2, many existing methods rely on such mechanisms, including: incrementally allocating new network resources for new tasks, augmenting the representation

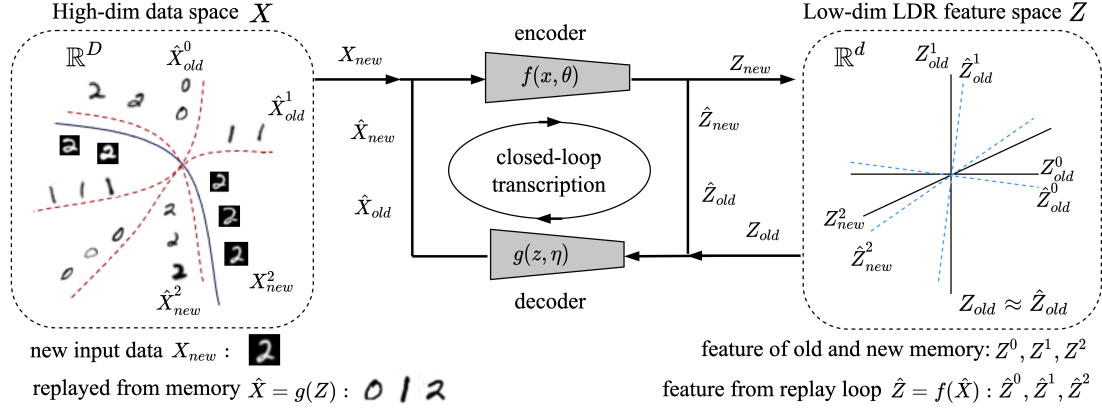


Figure 1. Overall framework of our closed-loop transcription based incremental learning for a structured LDR memory. Only a single, entirely self-contained, encoding-decoding network is needed: for a new data class X_{new} , a new LDR memory Z_{new} is incrementally learned as a minimax game between the encoder and decoder subject to the constraint that old memory of past classes Z_{old} is intact through the closed-loop transcription (or replay): $Z_{old} \approx \hat{Z}_{old} = f(g(Z_{old}))$.

heuristics or add hidden costs.

These two qualities additionally ensure that the self-contained neural system that incremental learning (IL) is conducted on also supports conventional *joint learning* (JL) methods, which learn all classes together. Incremental learning, however, can be much less demanding in terms of data preparation and computation than joint learning.²

In this work, we demonstrate that a framework based on *closed-loop transcription* (Figure 1) can mitigate catastrophic forgetting and outperform prior approaches to incremental learning, while achieving the qualities described above. Our paper includes studies on two key contributions: (1) how constrained data transcription can enable neural systems capable of graceful forgetting and (2) how a weakly supervised *incremental reviewing* process can further improve the learned memory.

Graceful forgetting via constrained data transcription. We show that the recently proposed closed-loop data transcription system (Dai et al., 2021) for learning a linear discriminative representation (LDR) of multiple object classes has the ability to avoid catastrophic forgetting in the above setting. The optimal LDR, which serves as the *structured memory* here, is learned jointly for all data classes through a minimax game between an encoder and decoder for an intrinsic rate reduction objective (Chan et al., 2021). In this work, we show that such a multi-class LDR can be effectively learned in an incremental setting too! The only thing one needs to modify is to optimize the (same) rate reduction objective for a new task *while trying to keep the learned LDR (memory) of the old classes intact*. Incremental learning thus reduces to a “controlled” representation learning

spaces, duplicating old networks while learning new ones, or explicitly identifying and isolating used/unused parts of the network.

²This often is not the case for many existing incremental learning methods, see Table 1 in Section 4 for an example.

task; computationally, instead of solving a minimax game (see eqn. (5)) when joint learning for all classes, incremental learning solves a *constrained minimax game* (see eqn. (8)).

The closed-loop encoding-decoding architecture and the rate reduction-based objective together provide a simple and unifying framework for incremental learning. As we demonstrate with experimental results (Section 4), they seem to be precisely the key elements needed to alleviate catastrophic forgetting, offering a direct answer to the aforementioned stability-plasticity challenge (Grossberg, 1987). Our experiments show that both the discriminative and generative properties of the incrementally learned LDRs degrade *gracefully*, typically significantly better than the state of the art incremental learning methods (see Table 2 and 3 in Section 4), despite lower resource requirements.

Incremental reviewing for jointly-optimal memory. As a neural system with a fixed capacity incrementally learns more classes, the memory of previously learned classes inevitably will degrade. If the raw data for an object class is seen only once, we can only expect to form a temporary memory. However, graceful forgetting secures a chance for the neural system to further consolidate the memory by reviewing the previously learned classes again. With the proposed framework, we show that memory improves even if this review process is *weakly supervised*: the system can review an old class without its class information as if it was learning a new one by optimizing exactly the same learning objective! After several review cycles, the final incrementally learned LDR achieves performance close to that obtained by learning all classes jointly (see Table 4). Our results suggest that *graceful forgetting* and *incremental reviewing* serve as two key computational mechanisms for an artificial system to form *jointly-optimal* memory for all classes.

2. Related Work

A large body of work has studied methods for addressing the incremental learning problem. In this section, we discuss a selection of representative approaches, and highlight their relationships to our approach.

In terms of *how new data classes are provided and tested*, incremental learning methods in the literature can be roughly divided into two groups: The first is *task* incremental learning (task-IL), where a model is sequentially trained on multiple tasks where each task may contain multiple classes to learn. At test time, the system is asked to classify data seen so far, *provided with a task-ID indicating which task the test data is drawn from*. Recently, more methods attempt to tackle *class* incremental learning (class-IL), which is similar to task-IL but does not require a task-ID at inference. Class-IL is therefore more challenging, and is the setting considered by this work.

In terms of *what information incremental learning relies on*, existing methods mainly fall into the following categories.

Regularization-based methods introduce penalty terms designed to mitigate forgetting of previously trained tasks. For instance, Elastic Weight Consolidation (EWC) (Kirkpatrick et al., 2017) and Synaptic Intelligence (SI) (Zenke et al., 2017) limit changes of model parameters deemed to be important for previous tasks by imposing a surrogate loss. Alternatively, learning without Forgetting (LwF) (Li & Hoiem, 2017) utilizes a knowledge distillation loss to prevent large drifts of the model weights during training on the current task. Although these methods, which all apply regularization on network parameters, have demonstrated competitive performance on task-IL scenarios, their performance does not transfer to the more challenging class-IL settings, as we show in our evaluations (Table 2).

Architecture-based methods explicitly alter the network architecture to incorporate new classes of data. Methods such as Progressive Neural Networks (PNN) (Rusu et al., 2016), Dynamically Expandable Representation (DER) (Yan et al., 2021) and ReduNet (Wu et al., 2021) add new neural modules to the existing network when required to learn a new task. Since these methods are not dealing with a single network with a fixed capacity, one disadvantage of these methods is therefore their memory footprint: their model size often grows linearly with the number of tasks or classes. Alternatively, other methods such as Progress & Compress (P&C) (Schwarz et al., 2018a), Packnet (Mallya & Lazebnik, 2018), and CLNP (Golkar et al., 2019) deal with one network with a fixed size but artificially divide the model parameters into different subsets for each task. Nevertheless, their learning performance tends to suffer once facing a large number of tasks. Additionally, most architecture-based methods target the less challenging task-IL problems and are not so suited for class-IL settings. In contrast, our work addresses the class-IL setting with only a simple, off-

the-shelf 4-layer network (see Appendix B for details).

Exemplar-based methods attempt to combat forgetting by explicitly retaining data from previously learned tasks. Most early memory-based methods, such as iCaRL (Rebuffi et al., 2017) and ER (Chaudhry et al., 2019), store a subset of raw data samples from each learned class, which is used along with the new classes to jointly update the model. A-Gem (Chaudhry et al., 2018) also relies on storing such an exemplar set but, rather than directly training with new data, it calculates a reference gradient from the stored data and projects the gradient from the new task onto these reference directions in hope of maintaining performance on old tasks. However, storing raw data of learned classes is neither resource-efficient nor natural from a neuroscientific perspective (Robins, 1995).

Generative memory-based methods utilize generative models such as GANs or autoencoders for replaying data for old tasks or classes, rather than storing raw samples and exemplars. Methods such as Deep Generative Replay (DGR) (Shin et al., 2017), Memory Replay Gans (MeRGAN) (Wu et al., 2018), and Dynamic Generative Memory (DGM) (Ostapenko et al., 2019) propose to train a GAN on previously seen classes and use synthesized data to alleviate forgetting when training on new tasks. To further improve memory efficiency, methods such as Farnet (Kemker & Kanan, 2018) and EEC (Ayub & Wagner, 2020) store intermediate features of old classes and use these more compact representations for generative replay. Existing generative memory-based approaches have performed competitively on class-IL without storing raw data samples, but require separate networks and feature representations for generative and discriminative purposes.

Like these works, our approach also takes a generative memory-based approach to incremental learning. However, we do so with only a single closed-loop encoding-decoding network. This closed-loop generative model is more stable to train (Dai et al., 2021), and enables a single, unified feature representation that serves both generative and discriminative purposes. There is no need to train separate generative and classifying networks. As a result, our method is much more resource-efficient than its joint setting; it is simpler yet more effective than existing methods.

3. Our Method

3.1. Linear Discriminative Representation as Memory

Consider the task of learning to memorize k classes of objects from images. WLOG, we may assume that images of each class belong to a low-dimensional submanifold in the space of images \mathbb{R}^D , denoted as \mathcal{M}_j , for $j = 1, \dots, k$. Typically, we are given a set of n samples $\mathbf{X} = [\mathbf{x}^1, \dots, \mathbf{x}^n] \subset \mathbb{R}^{D \times n}$ that are partitioned into k subsets $\mathbf{X} = \bigcup_{j=1}^k \mathbf{X}_j$, with each subset \mathbf{X}_j sampled from \mathcal{M}_j , $j = 1, \dots, k$. The goal here is to learn a compact rep-

resentation, or a “memory”, of these k classes from these samples, which can be used for both discriminative (e.g. classification) and generative purposes (e.g. replay).

Autoencoding. We model such a memory with an *autoencoding* tuple $\{f, g, z\}$ that consists of an encoder $f(\cdot, \theta)$, parameterized by θ , that maps the data $\mathbf{x} \in \mathbb{R}^D$ continuously to a compact feature \mathbf{z} in a much lower-dimensional space \mathbb{R}^d , and a decoder $g(\cdot, \eta)$, parameterized by η , that maps a feature \mathbf{z} back to the original data space \mathbb{R}^D :

$$f(\cdot, \theta) : \mathbf{x} \mapsto \mathbf{z} \in \mathbb{R}^d; \quad g(\cdot, \eta) : \mathbf{z} \mapsto \hat{\mathbf{x}} \in \mathbb{R}^D. \quad (1)$$

For the set of samples \mathbf{X} , we let $\mathbf{Z} = f(\mathbf{X}, \theta) \doteq [\mathbf{z}^1, \dots, \mathbf{z}^n] \subset \mathbb{R}^{d \times n}$ with $\mathbf{z}^i = f(\mathbf{x}^i, \theta) \in \mathbb{R}^d$ be the set of corresponding features. Similarly let $\hat{\mathbf{X}} \doteq g(\mathbf{Z}, \eta)$ be the decoded data from the features. The autoencoding tuple can be illustrated by the following diagram:

$$\mathbf{X} \xrightarrow{f(\mathbf{x}, \theta)} \mathbf{Z} \xrightarrow{g(\mathbf{z}, \eta)} \hat{\mathbf{X}}. \quad (2)$$

We may refer to such a learned tuple: $\{f(\cdot, \theta), g(\cdot, \eta), \mathbf{Z}\}$ as a compact “memory” for the given dataset \mathbf{X} .

Structured LDR autoencoding. For such a memory to be convenient to use for subsequent tasks, including incremental learning, we would like a representation \mathbf{Z} that has well-understood structures and properties. Recently, Chan *et al.* (2021) proposed that for both discriminative and generative purposes, \mathbf{Z} should be a *linear discriminative representation* (LDR). More precisely, let $\mathbf{Z}_j = f(\mathbf{X}_j, \theta)$, $j = 1, \dots, k$ be the set of features associated with each of the k classes. Then each \mathbf{Z}_j should lie on a low-dimensional linear subspace \mathcal{S}_j in \mathbb{R}^d which is highly incoherent (ideally orthogonal) to others \mathcal{S}_i for $i \neq j$. Notice that the linear subspace structure enables both interpolation and extrapolation, and incoherence between subspaces makes the features discriminative for different classes. As we will see, these structures are also easy to preserve when incrementally learning new classes.

3.2. Learning LDR via Closed-loop Transcription

As has been shown in (Yu *et al.*, 2020), such incoherent linear properties of the learned (LDR) features $\mathbf{Z} = f(\mathbf{X}, \theta)$ can be promoted by maximizing a coding rate reduction objective, known as the *MCR² principle*:

$$\max_{\theta} \Delta R(\mathbf{Z}) = \Delta R(\mathbf{Z}_1, \dots, \mathbf{Z}_k) \doteq \underbrace{\frac{1}{2} \log \det(\mathbf{I} + \alpha \mathbf{Z} \mathbf{Z}^*)}_{R(\mathbf{Z})} - \sum_{j=1}^k \underbrace{\gamma_j \frac{1}{2} \log \det(\mathbf{I} + \alpha_j \mathbf{Z}_j \mathbf{Z}_j^*)}_{R(\mathbf{Z}_j)},$$

where, for a prescribed quantization error ϵ , $\alpha = \frac{d}{n\epsilon^2}$, $\alpha_j = \frac{d}{|\mathbf{Z}_j|\epsilon^2}$, $\gamma_j = \frac{|\mathbf{Z}_j|}{n}$.

As noted in (Yu *et al.*, 2020), maximizing the rate reduction promote learned features that span the entire feature space. It is therefore not suitable to naively apply for the case of incremental learning, as the number of classes increases

within a fixed feature space.³ The closed-loop transcription framework introduced by (Dai *et al.*, 2021) suggests resolving such difficulties by suggesting learning the encoder $f(\cdot, \theta)$ and decoder $g(\cdot, \eta)$ together as a minimax game: while the encoder tries to maximize the rate reduction objective, the decoder should minimize it instead. That is, the decoder g minimizes resources (measured by the coding rate) needed for the replayed data for each class $\hat{\mathbf{X}}_j = g(\mathbf{Z}_j, \eta)$, decoded from the learned features $\mathbf{Z}_j = f(\mathbf{X}_j, \theta)$, to emulate the original data \mathbf{X}_j well enough. As it is typically difficult to directly measure the similarity between \mathbf{X}_j and $\hat{\mathbf{X}}_j$, (Dai *et al.*, 2021) proposes measuring this similarity with the *rate reduction* of their corresponding features \mathbf{Z}_j and $\hat{\mathbf{Z}}_j = f(\hat{\mathbf{X}}_j(\theta, \eta), \theta)$:

$$\Delta R(\mathbf{Z}_j, \hat{\mathbf{Z}}_j) \doteq R(\mathbf{Z}_j \cup \hat{\mathbf{Z}}_j) - \frac{1}{2}(R(\mathbf{Z}_j) + R(\hat{\mathbf{Z}}_j)). \quad (3)$$

The resulting ΔR gives a principled “distance” between subspace-Gaussian like ensembles, with the property that $\Delta R(\mathbf{Z}_j, \hat{\mathbf{Z}}_j) = 0$ iff $\text{Cov}(\mathbf{Z}_j) = \text{Cov}(\hat{\mathbf{Z}}_j)$ (Ma *et al.*, 2007).

Now considering all k classes together, we have two sets of features: the features $\mathbf{Z} = f(\mathbf{X}, \theta)$ for the original data \mathbf{X} and those $\hat{\mathbf{Z}} = f(\hat{\mathbf{X}}(\theta, \eta), \theta)$ for replayed data $\hat{\mathbf{X}} = g(\mathbf{Z}(\theta), \eta)$, through a “closed-loop” transcription:

$$\mathbf{X} \xrightarrow{f(\mathbf{x}, \theta)} \mathbf{Z} \xrightarrow{g(\mathbf{z}, \eta)} \hat{\mathbf{X}} \xrightarrow{f(\mathbf{x}, \theta)} \hat{\mathbf{Z}}. \quad (4)$$

Then by combining the above two rate reduction objectives, (Dai *et al.*, 2021) has shown that by solving the following *minimax program*:

$$\min_{\theta} \max_{\eta} \Delta R(\mathbf{Z}) + \Delta R(\hat{\mathbf{Z}}) + \sum_{j=1}^k \Delta R(\mathbf{Z}_j, \hat{\mathbf{Z}}_j), \quad (5)$$

one can learn a good LDR \mathbf{Z} when optimized jointly for all k classes. The learned representation \mathbf{Z} has clear incoherent linear subspace structures in the feature space which makes them very convenient to use for subsequent tasks (both discriminative and generative).

3.3. Incremental Learning with an LDR Memory

The incoherent linear structures for features of different classes closely resemble neural signals observed in different areas of the inferotemporal cortex of animal brains (Chang & Tsao, 2017; Bao *et al.*, 2020). The closed-loop transcription $\mathbf{X} \rightarrow \mathbf{Z} \rightarrow \hat{\mathbf{X}} \rightarrow \hat{\mathbf{Z}}$ also resembles popularly hypothesized mechanisms for memory formation (Ven *et al.*, 2020; Josselyn & Tonegawa, 2020). This leads to a natural question: since memory in the brains is formed in an incremental fashion, can the closed-loop transcription framework also support incremental learning?

LDR memory sampling and replaying. The simple linear structures of LDR make it extremely suitable for incremental learning: distribution of features \mathbf{Z}_j of each previously

³As the number of classes is initially small in the incremental setting, if the dimension of the feature space d is high, maximizing the rate reduction may over-estimate the dimension of each class.

learned class can be explicitly and concisely represented by a principal subspace \mathcal{S}_j in the feature space. To preserve the memory of an old class j , we only need to preserve the subspace while learning new classes. To this end, we simply sample m representative prototype features on the subspace along its top r principal components, and denote these features as $\mathbf{Z}_{j,old}$.⁴ Suppose a total of t old classes have been learned so far. If all of those prototype features, denoted $\mathbf{Z}_{old} \doteq [\mathbf{Z}_{old}^1, \dots, \mathbf{Z}_{old}^t]$, can be preserved when learning new classes, so will be all the subspaces $\{\mathcal{S}_j\}_{j=1}^t$ representing all past memory.

Notice that, with the learned auto-encoding (2), one can replay and use the images, say $\hat{\mathbf{X}}_{old} = g(\mathbf{Z}_{old}, \eta)$, associated with the memory features to avoid forgetting while learning new classes. This is typically how a generative model has been used for most incremental learning methods mentioned before. However, with the closed-loop framework, explicitly replaying images from the features is not necessary. Past memory can be effectively preserved through optimization exclusively on the features themselves, as we now explain.

Incremental learning LDR with old-memory constraint. Now let us consider the task of incrementally learning a new class of objects.⁵ We denote its new sample set as \mathbf{X}_{new} . The features of \mathbf{X}_{new} are denoted as $\mathbf{Z}_{new}(\theta) = f(\mathbf{X}_{new}, \theta)$. We concatenate them together with the prototype features of old classes \mathbf{Z}_{old} and form $\mathbf{Z} = [\mathbf{Z}_{new}(\theta), \mathbf{Z}_{old}]$. We denote the replayed images from all the features as $\hat{\mathbf{X}} = [\hat{\mathbf{X}}_{new}(\theta, \eta), \hat{\mathbf{X}}_{old}(\eta)]$ although we do not actually need to compute or use them explicitly. We only need features of those replayed images, denoted as $\hat{\mathbf{Z}} = f(\hat{\mathbf{X}}, \theta) = [\hat{\mathbf{Z}}_{new}(\theta, \eta), \hat{\mathbf{Z}}_{old}(\theta, \eta)]$. See Figure 1 for an illustration.

Following similar justification for the multi-class LDR objective (5), we would like the features of the new class \mathbf{Z}_{new} to be incoherent to all the old ones \mathbf{Z}_{old} . As \mathbf{Z}_{new} is the only new class whose features needs to be learned, the objective (5) reduces to the case $k = 1$:

$$\min_{\eta} \max_{\theta} \Delta R(\mathbf{Z}) + \Delta R(\hat{\mathbf{Z}}) + \Delta R(\mathbf{Z}_{new}, \hat{\mathbf{Z}}_{new}). \quad (6)$$

However, when we update the network parameters (θ, η) to optimize the features for the new class, the updated mappings f and g will change features of the old classes too. Hence, to minimize the distortion of the memory for old classes, we can try to enforce $\text{Cov}(\mathbf{Z}_{j,old}) = \text{Cov}(\hat{\mathbf{Z}}_{j,old})$. In other words, while learning new classes, we enforce the memory of old classes remain “self-consistent” through the transcription loop:

⁴In this work, we choose to represent the subspace with sampled features. Note that this is not the most compact representation for the subspace. Hence the storage footprint of our method has the potential of being further reduced!

⁵In Appendix A, we consider the more general setting where the task contains a small batch of new classes, and present all algorithmic details in that general setting.

$$\mathbf{Z}_{old} \xrightarrow{g(\mathbf{z}, \eta)} \hat{\mathbf{X}}_{old} \xrightarrow{f(\mathbf{x}, \theta)} \hat{\mathbf{Z}}_{old}. \quad (7)$$

Mathematically, this is equivalent to enforce $\Delta R(\mathbf{Z}_{old}, \hat{\mathbf{Z}}_{old}) \doteq \sum_{j=1}^t \Delta R(\mathbf{Z}_{j,old}, \hat{\mathbf{Z}}_{j,old}) = 0$. Hence, the above minimax program (6) needs to be revised to a *constrained* minimax game, which we refer to as *incremental LDR* (iLDR):

$$\begin{aligned} \min_{\eta} \max_{\theta} \quad & \Delta R(\mathbf{Z}) + \Delta R(\hat{\mathbf{Z}}) + \Delta R(\mathbf{Z}_{new}, \hat{\mathbf{Z}}_{new}) \\ \text{subject to} \quad & \Delta R(\mathbf{Z}_{old}, \hat{\mathbf{Z}}_{old}) = 0. \end{aligned} \quad (8)$$

Notice that, by comparing to the multi-class LDR objective (5), the constraint $\Delta R(\mathbf{Z}_{old}, \hat{\mathbf{Z}}_{old}) = 0$ is the only thing that we need to modify the original formulation.

In practice, the constrained minimax program can be solved by *alternating* minimization and maximization between the encoder $f(\cdot, \theta)$ and decoder $g(\cdot, \eta)$ as follows:

$$\begin{aligned} \max_{\theta} \quad & \Delta R(\mathbf{Z}) + \Delta R(\hat{\mathbf{Z}}) + \lambda \cdot \Delta R(\mathbf{Z}_{new}, \hat{\mathbf{Z}}_{new}) \\ & - \gamma \cdot \Delta R(\mathbf{Z}_{old}, \hat{\mathbf{Z}}_{old}), \end{aligned} \quad (9)$$

$$\begin{aligned} \min_{\eta} \quad & \Delta R(\mathbf{Z}) + \Delta R(\hat{\mathbf{Z}}) + \lambda \cdot \Delta R(\mathbf{Z}_{new}, \hat{\mathbf{Z}}_{new}) \\ & + \gamma \cdot \Delta R(\mathbf{Z}_{old}, \hat{\mathbf{Z}}_{old}); \end{aligned} \quad (10)$$

where the constraint $\Delta R(\mathbf{Z}_{old}, \hat{\mathbf{Z}}_{old}) = 0$ in (8) has been converted (and relaxed) to a Lagrangian term with a corresponding coefficient γ and sign. Here, we have introduced another coefficient λ for the rate reduction term associated with the new data to balance between old and new classes. More algorithmic details are given in Appendix A.

Incremental reviewing for a jointly-optimal memory. As we will see, the above constrained minimax program can already achieve state of the art performance for incremental learning. Nevertheless, developing an optimal memory for *all classes* cannot rely on graceful forgetting alone. Even for humans, if we learn one class of object only once, we should expect the learned memory will fade as we continue to learn new ones, unless the memory can be consolidated by reviewing old object classes repeatedly.

To emulate this phase of memory forming, after incrementally learning a whole dataset, we may go back to review all classes again, one class at a time. We refer to going through all classes once as one reviewing “cycle”.⁶ If needed, multiple reviewing cycles can be conducted. It is quite expected that reviewing can improve the learned (LDR) memory. But somewhat surprisingly, the closed-loop framework allows us to review even in a “class-unsupervised” manner: when reviewing data of an old class say \mathbf{X}_j , the system does not need the class label and can simply treat \mathbf{X}_j as a new class \mathbf{X}_{new} . That is, the system simply optimizes the same constrained mini-max program (8) without any modification!

⁶to distinguish from the term “epoch” used in the conventional joint learning setting.

After the system is optimized, one can simply identify the newly learned subspace spanned by Z_{new} , and use it to replace or merge with the old subspace S_j . As our experiments will show, such a weakly-supervised incremental review process can gradually improve both discriminative and generative performance of the LDR memory, eventually converging to that of a jointly-learned memory.

4. Experimental Verification

We now evaluate the performance of our method and compare with several representative incremental learning methods. Since different methods have very different requirements in data, networks, and computation, it is impossible to compare all in the same experimental conditions. For a fair comparison, we do not compare with methods that deviate significantly from the two qualities for IL that motivate our method: either methods that rely on feature extracting networks pre-trained on additional datasets such as Farnet (Kemker & Kanan, 2018) or methods that expand feature space and networks such as DER (Yan et al., 2021). For methods that we do compare against, we ensure that our method has a smaller model and memory footprint than alternative approaches.

4.1. Datasets, Networks, and Settings

Datasets. We conduct experiments on the following datasets: MNIST (LeCun et al., 1998), CIFAR-10 (Krizhevsky et al., 2014) and CIFAR-100 (Krizhevsky et al., 2009). All experiments are conducted for the more challenging class-IL setting. For both MNIST and CIFAR-10, the 10 classes are split into 5 tasks with 2 classes each or 10 tasks with 1 class each; for CIFAR-100, the 100 classes are split into 10 tasks of 10 classes each.

Simple four-layer networks. For all experiments presented in the main body, for the encoder f and decoder g , we adopt a very simple network architecture modified from DCGAN (Radford et al., 2016), which is merely a *four-layer* convolutional network. The details of architecture are given in Appendix B. The dimension d of the feature space is set accordingly for different datasets, $d=128$ for MNIST and CIFAR-10, $d=512$ for CIFAR-100.

More details about the algorithmic settings and ablation studies are given in the Appendix.

4.2. Comparison of Classification Performance

We first evaluate the LDR memory learned (without review) for classification.

A simple nearest subspace classifier. Similar to (Dai et al., 2021) and (Yu et al., 2020), we adopt a very simple *nearest subspace* algorithm to evaluate how discriminative our learned features are for classification. Suppose Z_j are the learned features of the j -th class. Let $\mu_j \in \mathbb{R}^d$ be its mean and $U_j \in \mathbb{R}^{d \times r_j}$ be the first r_j principal components for Z_j , where r_j is the estimated

dimension of class j . For a test data x' , its feature z' is given by $f(x', \theta)$. Then its class label will be predicted by $j' = \arg \min_{j \in \{1, \dots, k\}} \|(\mathbf{I} - U_j U_j^\top)(z' - \mu_j)\|_2^2$. It is especially noteworthy that our method does *not* need to train a separate deep neural network (based on the learned generative features) for classification whereas most other methods do.

Incremental learning versus joint learning. One main benefit of incremental learning is to learn one class (or one small task) at a time. So it should result in less storage and computation than jointly learning. Table 1 shows this is indeed the case for our method: IL on CIFAR-10 is 10 times faster than JL.⁷ However, this is often not the case for many existing incremental methods such as EEC (Ayub & Wagner, 2020), the current SOTA in generative memory-based methods. Not only does its incremental mode require a much larger model size (than its joint mode and ours⁸), it also takes significantly (7 times) longer to train.

Method	Resource	JL	IL	Diff
iLDR (ours)	Model Size	2 M	2 M	same
	Train Time	15 hours	1.5 hours	10x faster
EEC	Model Size	1 M	10 M	10x larger
	Train Time	0.6 hours	≥ 4 hours	7x slower

Table 1. The resource comparison on the joint learning (JL) and incremental learning (IL) of different methods. Both methods are tested on CIFAR-10 and the details of the comparison setting can be found in Appendix C.

MNIST and CIFAR-10. Table 2 compares our method against representative SOTA incremental learning methods in different categories on the MNIST and CIFAR-10 datasets. We report results for both 10-splits and 5-splits, in terms of both last accuracy and average accuracy (following definition in iCaRL (Rebuffi et al., 2017)). Results on regularization-based and exemplar-based methods are obtained by adopting the same benchmark and training protocol as in (Buzzeaga et al., 2020). All other results are based on publicly available code released by the original authors.

For a simple dataset like MNIST, we observe that our method outperforms all current SOTA on both settings. In the 10-task scenario, it is 1% higher on average accuracy, despite the SOTA is already as high as 97.8%. In general incremental learning methods achieve better performance for smaller number of steps. Here, our 10-step version even outperforms all other methods in the 5-step setting.

⁷Note in our method, both JL and IL optimize on the same network. The JL mode is trained on all ten classes together, hence it normally takes more epochs to converge and longer time to train. But the IL mode converges much faster, as it should have.

⁸For EEC, since its classifier and generators are separated, under the JL setting, it only needs a 8-layers convolutional network to train a classifier for all classes. In the incremental mode, it requires multiple generative models. Note that our JL model is also a generative model hence requires more time to train as well.

Category	Method	MNIST				CIFAR-10			
		10-splits		5-splits		10-splits		5-splits	
		Last	Avg	Last	Avg	Last	Avg	Last	Avg
Regularization	LwF (Li & Hoiem, 2017)	-	-	0.196	0.455	-	-	0.196	0.440
	oEWC (Schwarz et al., 2018b)	-	-	0.206	0.459	-	-	0.194	0.386
	SI (Zenke et al., 2017)	-	-	0.193	0.461	-	-	0.196	0.441
Architecture	ReduNet (Wu et al., 2021)	-	-	0.961	0.982	-	-	0.539	0.645
Exemplar (200 exemplars)	iCaRL (Rebuffi et al., 2017)	0.322	0.588	0.725	0.803	0.212	0.431	0.487	0.632
	ER (Chaudhry et al., 2019)	0.727	0.907	0.792	0.916	0.231	0.490	0.451	0.649
	A-GEM (Chaudhry et al., 2018)	0.382	0.574	0.597	0.764	0.115	0.293	0.204	0.473
Generative Memory	MeRGAN (Wu et al., 2018)	-	0.970	-	-	-	-	-	-
	DGMw (Ostapenko et al., 2019)	-	0.965	-	-	-	0.562	-	-
	EEC (Ayub & Wagner, 2020)	-	0.978	-	-	-	0.669	-	-
	EECS (Ayub & Wagner, 2020)	-	0.963	-	-	-	0.619	-	-
	iLDR (ours, 2K features)	0.974	0.988	0.978	0.990	0.594	0.720	0.607	0.716
	iLDR (ours, 5K features)	0.975	0.989	0.978	0.990	0.599	0.727	0.627	0.723

Table 2. Comparison on MNIST and CIFAR-10. “2/5 K features” means the number of features sampled for old classes during training. The storage size for 200 exemplars of CIFAR-10 is about 2.0 MB, compared to 0.97 MB for 2K features with 128 dimension.

For CIFAR-10, we observe more significant improvement. For incremental learning with more tasks (i.e splits = 10), to our best knowledge, EEC/EECS (Ayub & Wagner, 2020) represents the current SOTA. From the table, we see that even the smaller version of our our method outperforms EEC by more than 3%, despite the larger memory footprint that EEC’s multiple autoencoders require (see Table 1). For a more fair comparison, we have also included results of EECS from the same paper, which aggregate all autoencoders into one; our method outperforms EECS by nearly 10%. Also, we observe that our method with 10 steps is even better than all current methods that learn with 5 steps, in terms of both last and average accuracy. These results demonstrate the effectiveness of our approach.

CIFAR-100. We also evaluate and compare our method on CIFAR-100, which has a larger number of classes. The number of samples and features used is increased accordingly for all methods in this case. The results are reported in Table 3. Fewer methods are compared here because many generative memory-based methods are very difficult to scale up to many classes.⁹ In this experiment, we have set CIFAR-100 with 10-splits. From the table, we may see that even though our method uses learned features (not exemplars) and takes much less storage, it still outperforms other methods.

4.3. Generative Properties of the Learned LDR Memory

Unlike the incremental methods above, which learn models only for classification purposes (as those in Table 3), the closed-loop LDR model is both discriminative and generative. In this section, we show the generative abilities of our

⁹For example for CIFAR-100, the EEC method needs to be first trained on a batch of 50 classes, before trained incrementally (Ayub & Wagner, 2020).

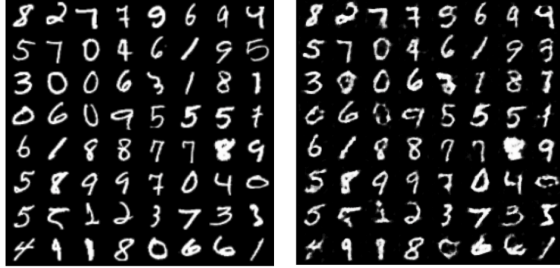
Method	Storage Size (MB)	Last
LwF	-	0.272
EWC	-	0.254
iCaRL (2K samples)	20.0 MB	0.346
BiC (2K samples)	20.0 MB	0.365
iLDR (ours, 5K features)	9.7 MB	0.385

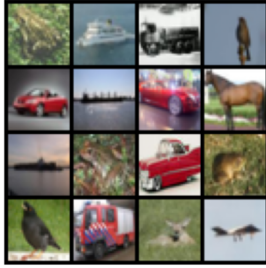
Table 3. Comparison on CIFAR-100. The feature dimension of iLDR on CIFAR-100 is 512. Hence, the storage size per feature for iLDR will 4 times larger than that on CIFAR-10.

model and visualize the structure of the learned memory.

Visualizing auto-encoding properties. We begin by qualitatively visualizing some representative images \mathbf{X} and the corresponding replayed $\hat{\mathbf{X}}$ on MNIST and CIFAR-10. The model is learned incrementally with the datasets split into 5 tasks. Results are shown in Figure 2, where we observe that the reconstructed $\hat{\mathbf{X}}$ preserves the main visual characteristics of \mathbf{X} including shapes, poses, and textures. For a simpler dataset like MNIST, the replayed $\hat{\mathbf{X}}$ are almost identical to the input \mathbf{X} ! This is rather remarkable given: (1) our method does not explicitly enforce $\hat{\mathbf{x}} \approx \mathbf{x}$ for individual samples as most autoencoding methods do, and (2) after having incrementally learned all classes, the generator has not forgotten how to generate digits learned earlier, such as 0, 1, 2. For a more complex dataset like CIFAR-10, iLDR also demonstrates good visual quality, faithfully capturing the essence of each image.

Principal subspaces of the learned features. Most generative memory-based methods utilize autoencoders, VAEs, or GANs for replay purposes. The structure or distribution of the learned features \mathbf{Z}_j for each class is unclear in the feature space. The features \mathbf{Z}_j of the LDR memory, on the other hand, have a clear linear structure. Figure 3 visualizes


 (a) MNIST \mathbf{X}

 (b) MNIST $\hat{\mathbf{X}}$

 (c) CIFAR-10 \mathbf{X}

 (d) CIFAR-10 $\hat{\mathbf{X}}$

Figure 2. Visualizing the auto-encoding property of the learned iLDR ($\hat{\mathbf{X}} = g \circ f(\mathbf{X})$) on MNIST, and CIFAR-10.

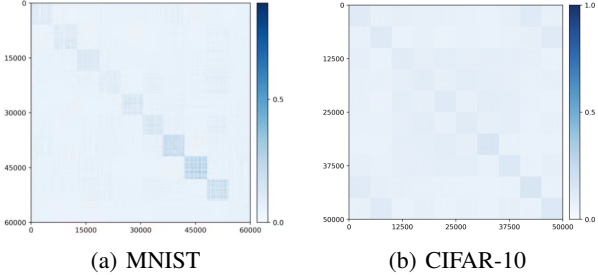
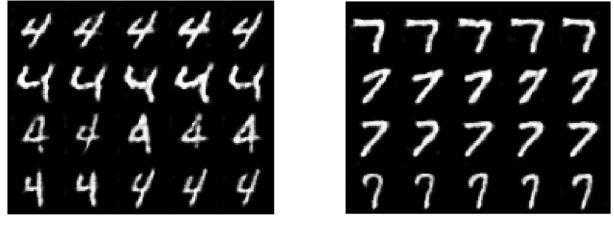


Figure 3. Block diagonal structure of $|\mathbf{Z}^T \mathbf{Z}|$ in the feature space for MNIST (left) and CIFAR-10 (right).

correlations among all learned features $|\mathbf{Z}^T \mathbf{Z}|$, in which we observe clear block-diagonal patterns for both datasets.¹⁰ This indicates the features for different classes \mathbf{Z}_j indeed lie on subspaces that are incoherent from one another. Hence, features of each class can be well modeled as a principal subspace in the feature space. A more precise measure of affinity among those subspaces can be found in Appendix D.

Replay images of samples from principal components. Since features of each class can be modeled as a principal subspace, we further visualize the individual principal components within each of those subspaces. Figure 4 shows the images replayed from sampled features along the top-4 principal components for different classes, on MNIST and CIFAR-10 respectively. Each row represents samples along

¹⁰Notice that these patterns closely resemble the similarity matrix of response profiles of object categories from different areas of the inferotemporal cortex, as shown in ExtendedDataFig.3 of (Bao et al., 2020).


 (a) sampled $\hat{\mathbf{x}}_{old}$ for ‘4’

 (b) sampled $\hat{\mathbf{x}}_{old}$ for ‘7’

 (c) sampled $\hat{\mathbf{x}}_{old}$ for ‘horse’

 (d) sampled $\hat{\mathbf{x}}_{old}$ for ‘ship’

Figure 4. Visualization of 5 reconstructed $\hat{\mathbf{x}} = g(\mathbf{z})$ from \mathbf{z} ’s with the closest distance to (top-4) principal components of learned features for MNIST (class ‘4’ and class ‘7’) and CIFAR-10 (class ‘horse’ and class ‘ship’), respectively.

one principal component and they clearly show similar visual characteristics but distinctively different from those in other rows. We see that the model remembers different types of ‘4’ or ‘7’ after having learned all remaining classes. For CIFAR-10, the incrementally learned memory remembers representative poses and shapes of horses and ships too.

4.4. Effectiveness of Incremental Reviewing

Last, we verify how the incrementally learned LDR memory can be further consolidated with an unsupervised incremental reviewing phase described at the end of Section 3.3. Experiments are conducted on CIFAR-10, with 10 steps.

Improving discriminativeness of the memory. Table 4 shows how the classification accuracy on all classes improves steadily after each cycle of incrementally reviewing the entire dataset. After a few (here 8) cycles, the accuracy approaches the same as that from learning all classes together in a joint fashion (last column).

# Rev. cycles	0	2	4	6	8	JL
Accuracy	0.599	0.626	0.642	0.650	0.658	0.655

Table 4. Classification accuracies for the overall test dataset after different numbers of review cycles on CIFAR-10.

Improving generative quality of the memory. Figure 5 left shows replayed images of the first class ‘airplane’ at the end of incremental learning of all ten classes, sampled along the top-3 principal components – every four rows (32 images) are along one principal direction. Their visual quality remains very decent – observed almost no forgetting. The

right figure shows replayed images after reviewing the first class once. We notice a significant improvement in visual quality after the reviewing, and principal components of the features in the subspace start to correspond to distinctively different visual attributes within the same class.

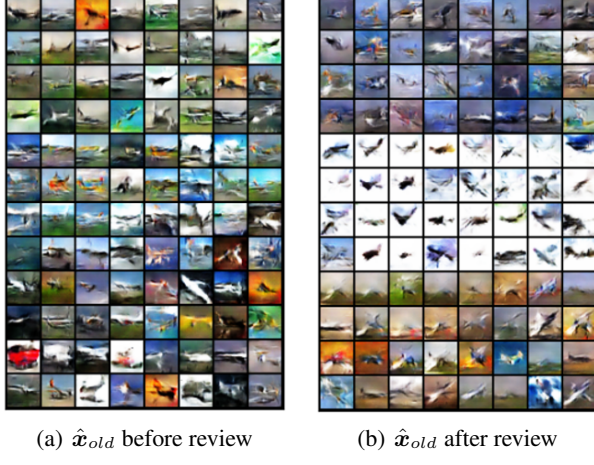


Figure 5. Visualization of replayed images \hat{x}_{old} of class 1-‘airplane’ in CIFAR-10, before and after one reviewing cycle.

5. Conclusion

This work provides a unifying framework that can incrementally learn a both discriminative and generative memory for multiple classes of objects. This is achieved through a closed-loop system with a feedback error measured by the information-theoretic rate reduction. Within such a closed-loop framework, the only difference between joint learning and incremental learning is that incremental learning solves a minimax game with an additional constraint that preserves (structures of) old memory. By combining the advantages of such a closed-loop transcription system and simple linear structures of the learned LDR memory, our method outperforms prior work and shows that both stability and plasticity can be achieved with *only a fixed-sized neural system and a single learning objective*. The simplicity of this new framework suggests there is tremendous potential that its performance, efficiency, and scalability can be significantly improved in future extensions.

6. Acknowledgements

Yi would like to thank Dr. Harry Shum for many stimulating discussions on incremental learning and interactive learning, and their importance to computer vision and computer graphics. We would like to thank Professor Doris Tsao of the Neuroscience Department at Berkeley for sharing with us her inspiring work and expertise on how memory of objects is organized and functions in the IT cortex of the brain. We also like to thank Professor Jack Gallant of the Neuroscience Department and Professor Claire Tomlin

of the EECS Department at Berkeley (and their teams) as this work is motivated from a joint ONR research project that aims to understand how memory is developed from perception and decision making and subsequently utilized for navigation purposes.

References

Allred, J. M. and Roy, K. Controlled forgetting: Targeted stimulation and dopaminergic plasticity modulation for unsupervised lifelong learning in spiking neural networks. *Frontiers in Neuroscience*, 14, 2020. ISSN 1662-453X. doi: 10.3389/fnins.2020.00007.

Ayub, A. and Wagner, A. EEC: Learning to encode and regenerate images for continual learning. In *International Conference on Learning Representations*, 2020.

Bao, P., She, L., McGill, M., and Tsao, D. Y. A map of object space in primate inferotemporal cortex. *Nature*, 583:103–108, 2020.

Buzzega, P., Boschini, M., Porrello, A., Abati, D., and Calderara, S. Dark experience for general continual learning: a strong, simple baseline. In *34th Conference on Neural Information Processing Systems (NeurIPS 2020)*, 2020.

Chan, K. H. R., Yu, Y., You, C., Qi, H., Wright, J., and Ma, Y. ReduNet: A white-box deep network from the principle of maximizing rate reduction. *CoRR*, abs/2105.10446, 2021. URL <https://arxiv.org/abs/2105.10446>.

Chang, L. and Tsao, D. The code for facial identity in the primate brain. *Cell*, 169:1013–1028.e14, 06 2017. doi: 10.1016/j.cell.2017.05.011.

Chaudhry, A., Ranzato, M., Rohrbach, M., and Elhoseiny, M. Efficient lifelong learning with a-gem. *arXiv preprint arXiv:1812.00420*, 2018.

Chaudhry, A., Rohrbach, M., Elhoseiny, M., Ajanthan, T., Dokania, P. K., Torr, P. H., and Ranzato, M. On tiny episodic memories in continual learning. *arXiv preprint arXiv:1902.10486*, 2019.

Dai, X., Tong, S., Li, M., Wu, Z., Chan, K. H. R., Zhai, P., Yu, Y., Psenka, M., Yuan, X., Shum, H. Y., and Ma, Y. Closed-loop data transcription to an LDR via minimaxing rate reduction. *arXiv preprint arXiv:2111.06636*, 2021.

Golkar, S., Kagan, M., and Cho, K. Continual learning via neural pruning. *arXiv preprint arXiv:1903.04476*, 2019.

Grossberg, S. Competitive learning: From interactive activation to adaptive resonance. *Cogn. Sci.*, 11:23–63, 1987.

Gulrajani, I., Ahmed, F., Arjovsky, M., Dumoulin, V., and Courville, A. Improved training of Wasserstein GANs. *arXiv preprint arXiv:1704.00028*, 2017.

Josselyn, S. A. and Tonegawa, S. Memory engrams: Recalling the past and imagining the future. *Science*, 367, 2020.

Kemker, R. and Kanan, C. FearNet: Brain-inspired model for incremental learning. In *International Conference on Learning Representations*, 2018.

Kingma, D. P. and Ba, J. Adam: A method for stochastic optimization. *arXiv preprint arXiv:1412.6980*, 2014.

Kirkpatrick, J., Pascanu, R., Rabinowitz, N., Veness, J., Desjardins, G., Rusu, A. A., Milan, K., Quan, J., Ramalho, T., Grabska-Barwinska, A., et al. Overcoming catastrophic forgetting in neural networks. *Proceedings of the national academy of sciences*, 114(13):3521–3526, 2017.

Krizhevsky, A., Hinton, G., et al. Learning multiple layers of features from tiny images. 2009.

Krizhevsky, A., Nair, V., and Hinton, G. The CIFAR-10 dataset. *online: http://www.cs.toronto.edu/kriz/cifar.html*, 55, 2014.

LeCun, Y., Bottou, L., Bengio, Y., Haffner, P., et al. Gradient-based learning applied to document recognition. *Proceedings of the IEEE*, 86(11):2278–2324, 1998.

Li, Z. and Hoiem, D. Learning without forgetting. *IEEE transactions on pattern analysis and machine intelligence*, 40(12):2935–2947, 2017.

Ma, Y., Derksen, H., Hong, W., and Wright, J. Segmentation of multivariate mixed data via lossy data coding and compression. *PAMI*, 2007.

Mallya, A. and Lazebnik, S. Packnet: Adding multiple tasks to a single network by iterative pruning. In *Proceedings of the IEEE conference on Computer Vision and Pattern Recognition*, pp. 7765–7773, 2018.

McCloskey, M. and Cohen, N. J. Catastrophic interference in connectionist networks: The sequential learning problem. In *Psychology of learning and motivation*, volume 24, pp. 109–165. Elsevier, 1989.

Ostapenko, O., Puscas, M., Klein, T., Jahnichen, P., and Nabi, M. Learning to remember: A synaptic plasticity driven framework for continual learning. In *Proceedings of the IEEE/CVF Conference on Computer Vision and Pattern Recognition*, pp. 11321–11329, 2019.

Radford, A., Metz, L., and Chintala, S. Unsupervised representation learning with deep convolutional generative adversarial networks. *arXiv preprint arXiv:1511.06434*, 2016.

Rebuffi, S.-A., Kolesnikov, A., Sperl, G., and Lampert, C. H. iCaRL: Incremental classifier and representation learning. In *Proceedings of the IEEE conference on Computer Vision and Pattern Recognition*, pp. 2001–2010, 2017.

Robins, A. V. Catastrophic forgetting, rehearsal and pseudorehearsal. *Connect. Sci.*, 7:123–146, 1995.

Rusu, A. A., Rabinowitz, N. C., Desjardins, G., Soyer, H., Kirkpatrick, J., Kavukcuoglu, K., Pascanu, R., and Hadsell, R. Progressive neural networks. *arXiv preprint arXiv:1606.04671*, 2016.

Schwarz, J., Czarnecki, W., Luketina, J., Grabska-Barwinska, A., Teh, Y. W., Pascanu, R., and Hadsell, R. Progress & compress: A scalable framework for continual learning. In *International Conference on Machine Learning*, pp. 4528–4537. PMLR, 2018a.

Schwarz, J., Czarnecki, W., Luketina, J., Grabska-Barwinska, A., Teh, Y. W., Pascanu, R., and Hadsell, R. Progress & compress: A scalable framework for continual learning. In *International Conference on Machine Learning*, pp. 4528–4537. PMLR, 2018b.

Shin, H., Lee, J. K., Kim, J., and Kim, J. Continual learning with deep generative replay. *arXiv preprint arXiv:1705.08690*, 2017.

Soltanolkotabi, M., Elhamifar, E., and Candes, E. J. Robust subspace clustering. *The Annals of Statistics*, 42(2):669–699, 2014.

Ven, G. M., Siegelmann, H. T., Tolias, A. S., et al. Brain-inspired replay for continual learning with artificial neural networks. *Nature Communications*, 11(1):1–14, 2020.

Wu, C., Herranz, L., Liu, X., van de Weijer, J., Raducanu, B., et al. Memory replay GANs: Learning to generate new categories without forgetting. *Advances in Neural Information Processing Systems*, 31:5962–5972, 2018.

Wu, Z., Baek, C., You, C., and Ma, Y. Incremental learning via rate reduction. In *Proceedings of the IEEE/CVF Conference on Computer Vision and Pattern Recognition*, pp. 1125–1133, 2021.

Yan, S., Xie, J., and He, X. DER: Dynamically expandable representation for class incremental learning. *arXiv preprint arXiv:2103.16788*, 2021.

Yu, Y., Chan, K. H. R., You, C., Song, C., and Ma, Y. Learning diverse and discriminative representations via the principle of maximal coding rate reduction. In *Advances in neural information processing systems*, 2020.

Zenke, F., Poole, B., and Ganguli, S. Continual learning through synaptic intelligence. In *International Conference on Machine Learning*, pp. 3987–3995. PMLR, 2017.

A. Algorithm Outline

For simplicity of presentation, the main body of this paper has described incremental learning with each incremental task containing one new class of data. In general, however, each incremental task may contain a finite C new classes. In this section, we detail the algorithms associated with iLDR in this more general setting.

Suppose we divide the overall task of learning multiple classes of data \mathcal{D} into a stream of smaller tasks $\mathcal{D}^1, \mathcal{D}^2, \dots, \mathcal{D}^t, \dots, \mathcal{D}^T$, where each task consists of labeled data $\mathcal{D}^t = \{\mathbf{X}^t, \mathbf{Y}^t\}$ from C classes, i.e., $\mathbf{X}^t = \{\mathbf{X}_1^t, \dots, \mathbf{X}_C^t\}$.

Prototype feature sampling. For each new task \mathcal{D}^t , the prototype set $\mathbf{Z}_{old} = [\mathbf{Z}_{old}^1, \dots, \mathbf{Z}_{old}^{t-1}]$ contains prototype features that are representative of subspaces for classes learned so far, sampled using PROTOTYPESAMPLING (Algorithm 1).

To seed this prototype set, we begin by training the model on the first task \mathcal{D}^1 , optimized via the original LDR objective function (5). We then use PROTOTYPESAMPLING to sample a prototype set of the classes in the first task. For simplicity, we choose to uniformly sample the principal subspace/components, although this scheme could be refined with importance sampling based on the (Gaussian) distribution in the subspace.

Notice in this work, we have chosen to use sampled features to represent and preserve the learned subspaces. This allows a learning objective to be formulated uniformly in terms of the rate reduction of features. Nevertheless, this requires a relatively large amount of storage for these features. Our formulation can certainly be improved by directly minimizing the distortion of the learned subspaces, which requires much less storage. We leave this for future investigation.

Incremental LDR (iLDR). The overall iLDR process is summarized in Algorithm 2. When learning a new task \mathcal{D}^t , we first draw a mini-batch of samples $(\mathbf{x}^t, \mathbf{y}^t)$ from it, and apply the model $\mathbf{x}^t \rightarrow \mathbf{z}^t \rightarrow \hat{\mathbf{x}}^t \rightarrow \hat{\mathbf{z}}^t$ to obtain \mathbf{z}^t and $\hat{\mathbf{z}}^t$. We then replay the old memory (prototype set) $\mathbf{Z}_{old} \rightarrow \hat{\mathbf{X}}_{old} \rightarrow \hat{\mathbf{Z}}_{old}$. So far, we get $\mathbf{Z} = [\mathbf{z}^t, \mathbf{Z}_{old}]$ and $\hat{\mathbf{Z}} = [\hat{\mathbf{z}}^t, \hat{\mathbf{Z}}_{old}]$. The new memory and old memory are optimized jointly to simultaneously create the new memory and preserve the old memory. The encoder updates θ by optimizing the objective (9):

$$\max_{\theta} \Delta R(\mathbf{Z}) + \Delta R(\hat{\mathbf{Z}}) + \lambda \Delta R(\mathbf{z}^t, \hat{\mathbf{z}}^t) - \gamma \Delta R(\mathbf{Z}_{old}, \hat{\mathbf{Z}}_{old}).$$

The decoder updates η via optimizing the objective (10):

$$\min_{\eta} \Delta R(\mathbf{Z}) + \Delta R(\hat{\mathbf{Z}}) + \lambda \Delta R(\mathbf{z}^t, \hat{\mathbf{z}}^t) + \gamma \Delta R(\mathbf{Z}_{old}, \hat{\mathbf{Z}}_{old}).$$

We optimize these objectives until the parameters converge. After the training session ends, prototypes of newly acquired

classes are stored into the prototype set, again with PROTOTYPESAMPLING. The process of training a new task and updating prototype set is repeated until all tasks are learned.

Algorithm 1 PROTOTYPESAMPLING(\mathbf{Z}^t, m, r)

input C classes of features $\mathbf{Z}^t = [\mathbf{Z}_1^t, \mathbf{Z}_2^t, \dots, \mathbf{Z}_C^t]$ of the entire t -th task, $t \in [1, \dots, T]$. The parameters m and r , which correspond to top- m features on each of top- r eigenvectors we will sample on each class;

- 1: **for** $j = 1, 2, \dots, C$ **do**
- 2: Calculate the top- r eigenvectors \mathbf{V}^j of \mathbf{Z}_j^t . $\mathbf{V}^j = [v_1, \dots, v_r]$ where v_n means the n -th eigenvector;
- 3: **for** $i = 1, 2, \dots, r$ **do**
- 4: Calculate projection distance $\mathbf{d} = v_i^\top \mathbf{Z}_j^t$;
- 5: Choose the top- m features from \mathbf{Z}_j^t based on the distance \mathbf{d} to form the set \mathbf{P}_i .
- 6: **end for**
- 7: Obtain prototype of j -th class $\mathbf{B}_j \doteq [\mathbf{P}_1, \dots, \mathbf{P}_r]$;
- 8: **end for**
- 9: Prototype set for t -th task $\mathbf{Z}_{old}^t \doteq [\mathbf{B}_1, \dots, \mathbf{B}_C]$.

output \mathbf{Z}_{old}^t

Algorithm 2 iLDR

input A stream of tasks $\mathcal{D}^1, \mathcal{D}^2, \dots, \mathcal{D}^T$; A pre-trained encoder $f(\cdot, \theta)$ and decoder $g(\cdot, \eta)$ on \mathcal{D}^1 ;

- 1: Initialize the prototype set \mathbf{Z}_{old} ;
- 2: **for** $t = 2, \dots, T$ **do**
- 3: $\mathbf{Z}_{old}^{t-1} = \text{PROTOTYPESAMPLING}(f(\mathbf{Z}_{old}^{t-1}), m, r)$;
- 4: Append \mathbf{Z}_{old}^{t-1} to $\mathbf{Z}_{old} = [\mathbf{Z}_{old}^1, \dots, \mathbf{Z}_{old}^{t-1}]$;
- 5: **while** not converged **do**
- 6: Draw samples $(\mathbf{x}^t, \mathbf{y}^t)$ from the t -th task \mathcal{D}^t ;
- 7: Compute expressions: $\mathbf{x}^t \rightarrow \mathbf{z}^t \rightarrow \hat{\mathbf{x}}^t \rightarrow \hat{\mathbf{z}}^t$;
- 8: Replay the old memory $\mathbf{Z}_{old} \rightarrow \hat{\mathbf{X}}_{old} \rightarrow \hat{\mathbf{Z}}_{old}$;
- 9: $\mathbf{Z} = [\mathbf{z}^t, \mathbf{Z}_{old}]$; $\hat{\mathbf{Z}} = [\hat{\mathbf{z}}^t, \hat{\mathbf{Z}}_{old}]$;
- 10: Update θ via the optimization objective (9);
- 11: Update η via the optimization objective (10);
- 12: **end while**
- 13: **end for**

output $f(\cdot, \theta)$ and $g(\cdot, \eta)$

B. Implementation Details

A simple network architecture. Table 5 and 6 give details of the network architecture for the decoder and the encoder networks used for experiments reported in Section 4. All α values in Leaky-ReLU (i.e. lReLU) of the encoder are set to 0.2. We set ($nz = 128$ and $nc = 1$) for MNIST, ($nz = 128$ and $nc = 3$) for CIFAR-10, ($nz = 512$ and $nc = 3$) for CIFAR-100.

Optimization settings. For all experiments, we use Adam (Kingma & Ba, 2014) as our optimizer, with hyperparam-

$z \in \mathbb{R}^{1 \times 1 \times nz}$
4×4 , stride=1, pad=0 deconv. BN 256 ReLU
4×4 , stride=2, pad=1 deconv. BN 128 ReLU
4×4 , stride=2, pad=1 deconv. BN 64 ReLU
4×4 , stride=2, pad=1 deconv. 1 Tanh

Table 5. Network architecture of the decoder $g(\cdot, \eta)$.

Image $x \in \mathbb{R}^{32 \times 32 \times nc}$
4×4 , stride=2, pad=1 conv 64 IReLU
4×4 , stride=2, pad=1 conv. BN 128 IReLU
4×4 , stride=2, pad=1 conv. BN 256 IReLU
4×4 , stride=1, pad=0 conv nz

Table 6. Network architecture of the encoder $f(\cdot, \theta)$.

ters $\beta_1 = 0.5$, $\beta_2 = 0.999$. Learning rate is set to be 0.0001. We choose $\epsilon^2 = 1.0$, $\gamma = 1$, and $\lambda = 10$ for both equation (9) and (10) in all experiments. Each task is trained for 120 epochs. All experiments are conducted with 1 or 2 RTX 3090 GPUs.

C. The Setting of Resource Comparison

In Table 1 of the main body, both iLDR and EEC methods are tested on CIFAR-10. Under joint learning, LDR follows the setting in the Appendix A.4 of (Dai et al., 2021). But we adopt the architectures of the encoder and decoder detailed in Table 6 and Table 5, respectively. The training batch size is 1600 with 1400 epochs because the generative LDR model is generally more challenging to train than a simple classifier network as EEC does in the joint learning setting. For EEC, it uses the ResNet architecture from (Gulrajani et al., 2017) for the classifier, and its training batch size and training epochs are 128 and 100 respectively.

D. Affinity between Learned Subspaces

As we have seen in Figure 3, the learned features of different classes are highly incoherent and their correlations form a block-diagonal pattern. We here conduct more quantitative analysis of the affinity among the subspaces learned for different classes. The analysis is done on features learned for CIFAR-10 using 10 splits with 2000 features. For two subspaces \mathcal{S} and \mathcal{S}' of dimension d and d' , we follow the definition of normalized affinity in (Soltanolkotabi et al., 2014):

$$\text{aff}(\mathcal{S}, \mathcal{S}') \doteq \sqrt{\frac{\sum_i^{d \times d'} \cos^2 \theta^i}{d \times d'}}. \quad (11)$$

We calculate the $\text{aff}(\mathcal{S}, \mathcal{S}')$ through $\|\mathbf{U}^\top \mathbf{U}'\|_F$ where \mathbf{U}/\mathbf{U}' is the normalized column space of features \mathbf{Z}/\mathbf{Z}' that can be obtained by SVD.

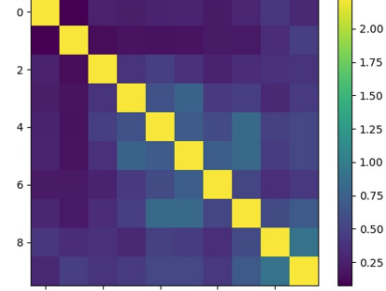


Figure 6. Affinity between memory subspaces within CIFAR-10.

The affinity measures the angle between two subspaces. The larger the value, the smaller the angle. As shown in Figure 6, we see that similar classes have higher affinities. For example, 8-ship and 9-trucks have higher affinity in the figure, whereas, 6-frogs has a much lower affinity to these two classes. This suggests that the affinity score of these subspaces captures similarity in visual attributes between different classes.

E. Ablation Studies

We conduct all ablation studies under the setting of CIFAR-10 split into 5 tasks with a feature size 2000. Set the default value for $m = 20$, $r = 12$, $\lambda = 10$, and $\gamma = 1$. We use the average incremental accuracy as a measure for the studies.

E.1. Impact of Choice of Optimization Parameters

Parameter m and r for memory sampling. Here we verify the impact of the memory size of Algorithm 1 on the performance of our method. The feature size is determined by two hyper-parameters r , which is the number of the PCA directions and m , which is the number of sampled features around each principal direction. The value of r varies from 10 to 14, and the value of m varies from 20 to 40. Table 7 reports the results of the average incremental accuracy. From the table, we observe that as long as the selection of m and r are in a reasonable range, the overall performance is stable.

	$m=20$	$m=30$	$m=40$
$r=10$	0.713	0.720	0.728
$r=12$	0.719	0.727	0.725
$r=14$	0.718	0.721	0.725

Table 7. Ablation study on varying m and r in PROTOTYPESAMPLING, in terms of the average incremental accuracy.

Hyper-parameter λ and γ in the learning objective. λ and γ are two important hyper-parameters in the objective functions for both (9) and (10). Here, we want to justify our selection on λ and γ and demonstrate the stability of our method to their choices. We analyze the sensitivity of the performance to the λ and γ respectively. In Table 8, we set

$\gamma = 1$ and change the value of λ from 0.1 to 50. The results indicate the accuracy becomes low only when λ are chosen to be extreme (e.g 0.1, 1, 50). We then change the value of γ in a large range from 0.01 to 100 with λ fixed at 10. Results in Table 9 indicate that the accuracy starts to drop when γ is larger than 10. Hence, in all our experiments reported in Section 4, we set $\lambda = 10$ and $\gamma = 1$ for simplicity.

λ	0.1	1	10	20	50
Accuracy	0.592	0.620	0.712	0.701	0.691

Table 8. Ablation study on varying λ in terms of the average incremental accuracy.

γ	0.01	0.1	1	10	100
Accuracy	0.713	0.716	0.712	0.700	0.655

Table 9. Ablation study on varying γ in terms of the average incremental accuracy.

E.2. Stability to Choice of Random Seeds

It is known that some incremental learning methods such as (Kirkpatrick et al., 2017) can be sensitive to random seeds. We report in Table 10 the average incremental accuracy of iLDR with different numbers of random seeds (conducted on CIFAR-10 split into 10 tasks, with a feature size 2000). As we can see, the choice of random seeds has very little effect on the performance.

# Random Seeds	1	5	10	15	100
Average Accuracy	0.720	0.720	0.720	0.720	0.721
Last Accuracy	0.594	0.592	0.593	0.594	0.594

Table 10. Ablation study on varying random seeds.